IOPscience iopscience.iop.org

Home Search Collections Journals About Contact us My IOPscience

Impact of GaP layer deposition upon photonic bandgap behaviour of opal

This article has been downloaded from IOPscience. Please scroll down to see the full text article.

2000 J. Phys.: Condens. Matter 12 339

(http://iopscience.iop.org/0953-8984/12/3/312)

View the table of contents for this issue, or go to the journal homepage for more

Download details:
IP Address: 171.66.16.218
The article was downloaded on 15/05/2010 at 19:33

Please note that terms and conditions apply.

J. Phys.: Condens. Matter **12** (2000) 339–348. Printed in the UK PII: S0953-8984(00)05298-X

Impact of GaP layer deposition upon photonic bandgap behaviour of opal

S G Romanov†‡, R M De La Rue†, H M Yates§ and M E Pemble§

† Optoelectronics Research Group, Department of Electronics and Electrical Engineering, University of Glasgow, Glasgow G12 8QQ, UK
‡ A F Ioffe Physical Technical Institute, St Petersburg, 194021, Russia
§ Department of Chemistry, University of Salford, Salford, M5 4WT, UK

E-mail: s.romanov@elec.gla.ac.uk

Received 17 June 1999, in final form 9 November 1999

Abstract. Thin (less than 4 nm thick) film layers of InP and GaP were deposited onto the inner surface of synthetic opal to enhance the refractive index contrast of this photonic crystal. The MOCVD process was deliberately modified to produce in-void chemical synthesis of compound semiconductors. The overall effect upon the photonic bandgap (PBG) behaviour appears to be large in coated opals as compared with bare opal. Apart from the 'red' shift of the stop-band in accordance with Bragg's law, the angular dispersion was found to be squeezed by nearly a factor of two, within the same range of angles of oblique light incidence, compared with bare opal. A trend has been demonstrated towards overlapping of the stop-bands over a wider range of directions in the photonic crystal as coating thickness increases. Improved overlap of the stop-bands results in the stronger suppression/enhancement of the spontaneous emission from GaP-coated opal as compared with bare opal.

1. Introduction

The design and study of three-dimensional (3D) photonic crystals operating at visible wavelengths is motivated by the promising applications for devices with controllable spontaneous emission [1]. Among the various work carried out, attention has been paid by a number of workers to developing colloidal crystals, and opals in particular, because their structure substantially meets the requirements for three-dimensional photonic crystals. Opals made from silica balls demonstrate an anisotropic photonic bandgap (PBG) associated with the 3D-periodic modulation of the dielectric properties in the ball package. Light scattered by opal shows a diffraction peak (Bragg resonance) at the observation wavelength which relates straightforwardly to the spacing of the balls in the package. By varying the ball diameter, this resonance can be anchored anywhere in the range from 200 to 1000 nm [2]. However, the shift of the resonance peak with changes in the direction of the optical propagation in the crystal clearly indicates the anisotropy of the optical properties of bare opal. The obvious reason for this anisotropy is the insufficiently deep refractive index (RI) modulation of the silica–air composite. Two ways of increasing the refractive index contrast (RIC) have been used: (i) impregnation of the interstitial voids of the opal package with high-RI material [3] and (ii) inversion of the ball package via impregnation of the voids with high-RI material and subsequent etching away of the balls [4, 5]. So far neither method has succeeded in producing a photonic crystal with an omnidirectional bandgap. With the first method it seems impossible

0953-8984/00/030339+10$30.00 © 2000 IOP Publishing Ltd

to approach the desired level of contrast because in a fully loaded opal the 'guest' material exhibits RIC with a silica (RI ∼1.45) background. The second method brings an extra level of disorder to the inverted structure due to partial collapse in the course of removal of the balls of the template—and substantial level of Rayleigh scattering.

Recently we have proposed to approach the problem of increasing the RIC in opals by replacing the silica–air interface with a semiconductor–air interface [6, 7]. If the internal surface of the opal voids is coated with a thin layer of high-RI semiconductor and some air is preserved in the opal voids, this approach gives a high RIC in relation to the low index background. This concept is undergoing extensive theoretical modelling to evaluate its PBG prospects [8, 9]—and the first experimental attempts have shown a promising improvement in the photonic bandgap properties of coated opals [7, 10, 11].

The choice of the semiconductor used for the coating is crucial in achieving photonic crystals with an operating range in the visible part of the spectrum. Materials combining the required high RI and a wide electronic bandgap are quite rare and GaP is one of the semiconductors which may open up this possibility. In this paper we report on the optical properties of GaP-coated opal and compare the optical properties of the GaP-coated opals with those of bare opal and InP-coated opal.

2. Materials

The silica balls which comprise the opal package are arranged in a face centred cubic (fcc) lattice, thus forming a 3D grating. Such a package contains empty voids of two distinct types: octahedral voids (O-voids) with a characteristic size of $d_O = 0.41D$ and tetrahedral voids (T-voids) with a size of $d_T = 0.23D$. These voids are interconnected, which allows the impregnation of the free opal volume with 'guest' material [12]. Opals with $D \approx 240$ nm and porosity $f_{Air} = 0.13$ and 0.23 were used. The semiconductor growth was carried out in opal by atmospheric pressure MOCVD, using phosphine (Linde) and trimethyl indium or trimethyl gallium (Epichem). The experimental method was modified from that usually used for MOCVD, with lower growth temperatures (maximum 350 °C) and alternative addition of the precursors, as opposed to the normal epitaxial growth of InP or GaP, where the precursors are present simultaneously. The GaP synthesis method is similar to that used in our previous work with InP [10]. In what follows we denote bare opal as air-opal and opal with InP and GaP coatings as InP-opal and GaP-opal.

The Raman spectra of InP- and GaP-filled opals were excited by the 514.5 nm line of an Ar-ion laser and collected in a backward scattering geometry (figure 1). The overall intensity of the Raman signal was very low, in accordance with there being a low volume fraction of semiconductor in the opal. In InP-opal the spectral maxima are centred at 294 and 345 cm^{-1}—and correspond closely to the TO (303 cm^{-1}) and LO (345 cm^{-1}) phonons of bulk InP. These bands are superimposed on the broad Raman band of partly ordered silica in an opal skeleton, which spreads between 300 and 500 cm^{-1}. A similar band has been resolved in the Raman spectra of naturally grown opals [13]. Usually, the Raman band of silica is obscured in the spectrum of opal because of the intense fluorescence of the oxygen vacancies in the silica, but in this case the defect-related fluorescence was suppressed due to the deposition of InP.

For GaP-opal it is hardly possible to resolve distinct Raman bands over the background formed by silica component of the nanocomposite (figure 1). By comparison with the Raman spectrum of silica extracted from the InP-opal spectrum, two bands centred at 365 and 407 cm^{-1} can be assigned to the TO (367 cm^{-1}) and LO (412 cm^{-1}) phonons of bulk GaP.

The main lesson to be learned from these spectra is that the deposited layer consists of semiconductor nanocrystallites. Apparently, this stage of the deposition process corresponds

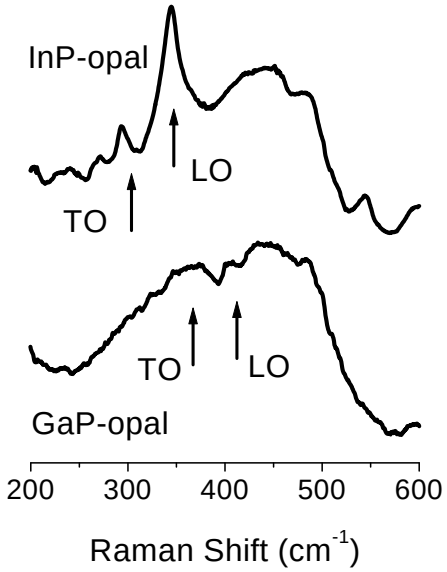

Figure 1. Raman spectra of opals coated with InP and GaP. LO and TO phonon frequencies in crystalline semiconductors are shown for reference.

to the formation of semiconductor clusters nucleating on centres of absorption on the surface of the silica skeleton of opal. The more intensive Raman spectrum of InP-opal can presumably be ascribed to the higher amount of semiconductor deposited in it than in GaP-opal.

3. Diffraction

Reflectance spectra were studied to characterize the Bragg diffraction from opal composites. They were measured at different angles θ_{inc} of incidence of the light with respect to the sample surface normal. Samples were in the shape of platelets $\sim$0.3 mm thick, with the (111) plane of the opal package oriented along the surface. The scattered light was collimated within 2° divergence before incidence on the detector to perform the angle-resolved measurements. For recording of the reflectance at oblique incidence, specular conditions were used ($\theta_{inc} = \theta_{scat}$ with respect to the surface normal).

The reflectance spectra of InP-opal and GaP-opal appear to be more complicated than the spectrum of air-opal. The shoulder in the spectrum of InP-opal at 1.3 eV and the shoulder at 2.35 eV for the GaP-opal reflectance correlate well with the absorption edge of the semiconductor component of the photonic crystals (figure 2). These features remain stationary for changes of the θ-angle. In contrast, the peak at 2.43 eV for InP-opal and 2.12 or 2.53 eV for GaP-opal can be assigned to the diffraction resonances, because they change their spectral position with changes in the angle of the light incidence in a similar manner to the diffraction peak from air-opal (figure 3). In what follows we assume that the Bragg peak corresponds to the stop-band in the PBG structure of the opal. Thus two different energy band structures contribute to the reflectance from the coated opals. The electronic band structure comes from the material of the photonic crystal while the photonic bandgap structure is due to the periodic changes of the dielectric constant. Of course, the electronic energy band structure of air-opal is also nontrivial, but the fundamental gap in silica is much wider than the energy range of the visible light. The remarkable feature of InP-coated opals is that the non-zero absorption does not destroy the PBG characteristics, so the interference between the electronic and photonic band structures can be neglected in the first instance.

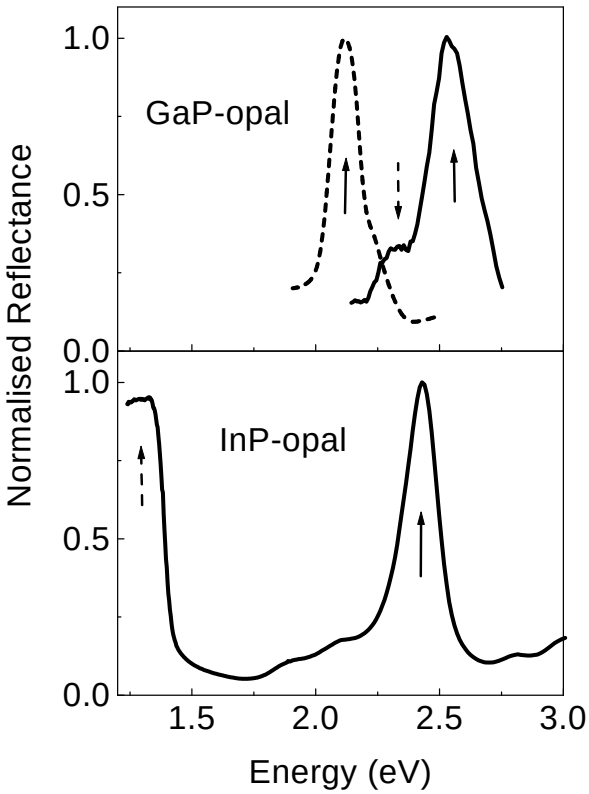

Figure 2. Reflectance spectra at $\theta = 5^\circ$ for (a) GaP-opals with $f_{SiO_2} = 0.87$ (dotted and solid lines, respectively) and (b) InP-opal $f_{SiO_2} = 0.77$. Diffraction resonance energies are indicated by the solid arrows and the electronic band-edge energies by dashed arrows.

The characteristics of the Bragg peak depend on several factors: the lattice constant of the photonic crystal, the amount of deposited semiconductor, the RI of the semiconductor, the direction of the optical propagation in the lattice and the polarization of the electromagnetic waves. The first factor is essentially trivial because of its simple scalability. The study of polarized reflectance is non-informative in the case of a textured polycrystalline opal. We assume that the spectra observed were averages over several randomly oriented areas of approximately 100 micron lateral dimensions. Correspondingly, we will focus our discussion on robust characteristics of semiconductor-coated opals like the opening of the stop-band in (111) direction and the spectral position of the stop-band.

The 'red' shift of the Bragg resonance in a loaded opal as compared with a bare opal occurs as a straightforward consequence of the increase of the average RI. From the Bragg law the resonance wavelength can be determined as $\lambda_B = 2n_{av}d$ [14], where d is the distance between the lattice planes, for light propagating normal to the plane of scattering. The average RI in accord with a simplified effective medium representation is given by $n_{av} \approx \sum_i n_i f_i$ the sum of the RIs, n_i, of the constituents of the photonic crystal weighted according to their volume fractions, f_i. All the samples were oriented with the (111) plane parallel to the platelet surface—and therefore d is the distance between the (111) planes of the fcc lattice. Because the linear dependence $\lambda_B \propto n_{av}$ applies both for bare and infilled opals with the same $d = 0.816D$,

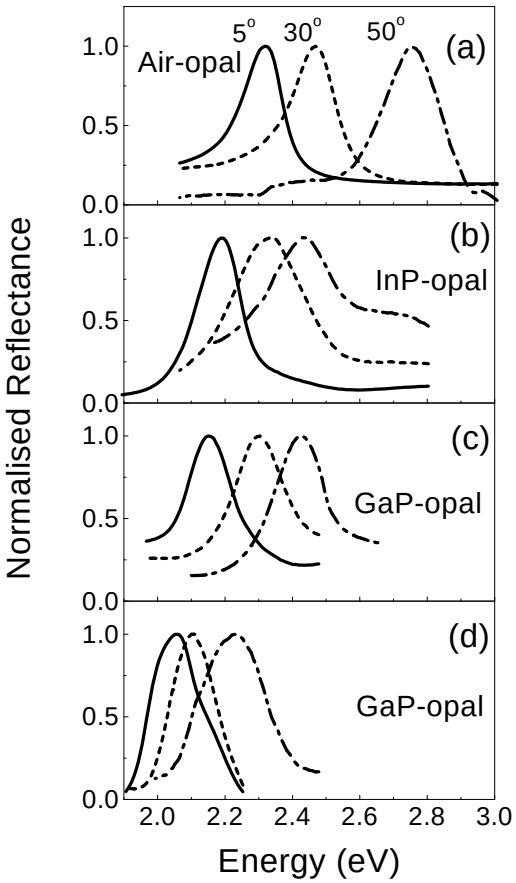

Figure 3. Bragg resonances at $\theta = 5^\circ$ (solid line), 30° (dot) and 50° (dash–dot) for (a) air-opal; (b) InP-opal; (c) GaP-opal with $f_{GaP} = 32\%$ and (d) $f_{GaP} = 7.3\%$, respectively. $f_{SiO_2} = 0.87$ for all samples applies. Peak resolution depends on the ordering of photonic crystal.

the estimate of the volume fraction of semiconductor can be obtained from the red shift of the Bragg resonance in coated opal as compared with bare opal. In figure 4(a), (b) the above proportionalities $n_{av} \propto f_{GaP}$ and $\lambda_B \propto f_{GaP}$ are revealed by plotting data for differently infilled opals.

The independent evaluation of the GaP content by standardless x-ray quantitative microanalysis (EDX) shows a lower amount of GaP than that extracted from the Bragg law, e.g. GaP-opal containing about 1 vol.% of semiconductor estimated by EDX demonstrates a red shift of the Bragg peak corresponding to 3.1 vol.% of GaP ($n_{GaP} = 3.42$ at $E = 2.3$ eV). This discrepancy is apparently due to the low filling factor of semiconductor and the instrumental uncertainty for EDX studies of porous dielectric media, where the continuous electron beam creates space charge which causes a much stronger effect upon the EDX data for the porous medium than for common solids [15]. Apparently, the use of a proper standard will improve the reliability of EDX data.

With changes in the GaP fraction, the width of the Bragg peak also increases (figure 4(c), where the full width at the half-height was used). However, for the 3.1 vol.% GaP filled opal the relative stopband width appears narrower than that in air-opal. The effect of the

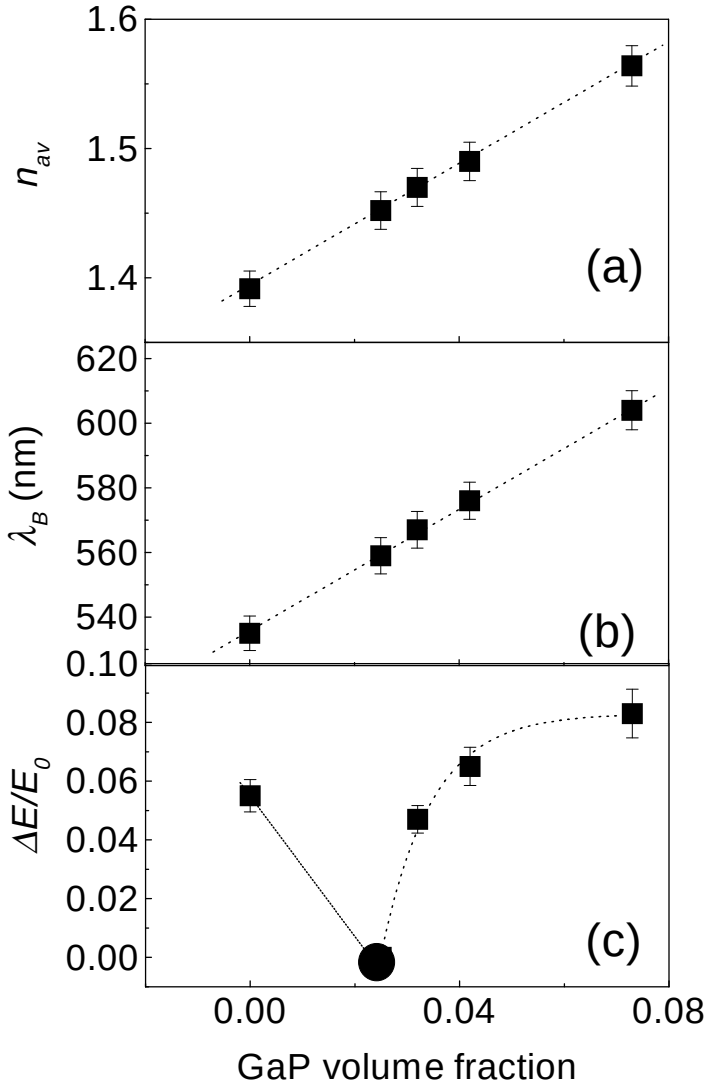

Figure 4. Dependences of (a) the effective RI, (b) wavelength of the Bragg resonance in (111) direction and (c) relative bandgap width at the L point of the Brillouin zone of GaP-opal upon the volume fraction of GaP coating. The circle in (c) corresponds to the assumed point of the bandgap collapse. Dotted lines show the linear (a), (b) and exponential (c) fits. Note the tendency for bandgap width saturation.

spherical shell places the effective RI of the coated void at a value intermediate between the RI of the coating and the RI of the air core [16]. When the RI of the silica ball matches that of the shell, the photonic bandgap disappears. From the standpoint of the effective medium approximation this matching point corresponds to ∼19% of the void being filled with GaP, or 2.5 vol.% for the GaP-opal with 13 vol.% porosity. This estimate, which is shown as the circle in figure 4(c), is in good agreement with the experimental data. The PBG collapse occurs at an approximately 4 nm thick semiconductor coating layer in the opal voids, a figure derived from simple geometrical considerations. We emphasize the relatively small increase in the bandgap

width resulting from the increase of loading. Moreover, as figure 4(c) shows, the saturation of the bandgap width upon the increase of the coating thickness is a very probable scenario. This result suggests that the RI contrast in studied composites is insufficient for opening an omnidirectional bandgap in accord with the theoretical prediction [9].

All the gratings studied, air-opal, InP-opal and GaP-opal, show a shift in the Bragg resonance to higher energies at increasing angles θ_{inc} of optical incidence (figure 3). However this shift is much smaller in coated opals than in air-opal. Moreover, the overlap of the stop-bands improves significantly with the increase of the opal loading (compare figures 3(c) and (d)). Squeezing of the angular dispersion of the stop-band in loaded opal has already been mentioned in the case of opal impregnated with sulphur [17] and with CdS [18]. The increase in the effective RI in coated opals (e.g. $n_{av} = 1.49$ for GaP-opal with $f_{GaP} = 4.2$ vol.%) is not too large to change significantly the angle of refraction as compared with air-opal ($n_{av} = 1.39$). Therefore, the apparent reason for a transformation of the angular dispersion is the inversion of the scattering ensemble, which is accompanied by a more complex spatial distribution of the electromagnetic field in coated opal. In particular, this problem was addressed in [17]. Detailed theoretical modelling of the light scattering in the directions other than the high-symmetry axes of an fcc crystal is required for a better understanding of this effect. By referring to the PBG structure of S-opal we can conclude that the semiconductor-coated opals demonstrate a similar effect on the angular dispersion of the stop-band to complete loading, i.e. a trend towards significant overlap of the stop-bands for different directions in the photonic crystal.

4. Photoluminescence

PL spectra were excited by the 2.41, 2.71 and 3.53 eV lines of an Ar-ion laser and the samples were cooled down to 5 K. To achieve a clear resolution of the impact of the stop-band upon the PL, the luminescence was collected from the sample surface on the opposite side to that exposed to the laser beam. The emission was collected from a solid angle of about 5° to resolve the angular variation of the PL spectrum. Under 2.71 eV excitation the PL of GaP-opal shows a broadband spectrum, the shape of which depends on the angle of collection of the light (figure 5(a)). In the case of opals lightly loaded with semiconductor, the PL signal consists of the recombination emission of the photoexcited defects (oxygen vacancies in the silica structure) of the opal skeleton and the emission due to electron–hole recombination in the semiconductor. In the PL spectrum of InP-opal these emission bands are well separated because the band which originates from the silica defects is centred at 2.2 eV, whereas the recombination in the semiconductor produces a band below 1.51 eV (figure 6(a)). The PL band of the air-opal (figure 6(b)) overlaps completely with the PL band of GaP-opal (figure 5(a)) when both are excited by the 2.71 eV line. Apparently, in the continuous wave regime of PL excitation, there is no way of separating the contributions from the template and the coating because: (i) the oxygen defects act as traps for electron–hole pairs generated in the semiconductor and (ii) the emission can be captured and then re-emitted. The actual PL band from the GaP coating centred at 2.1 eV is separated from the PL band of the silica defects when the 3.53 eV excitation line is used. This separation occurs because the emission band of the silica defects peaks at an energy slightly below the energy of the laser excitation, whereas the GaP band is unchanged (figure 6(a)) [6]. Moreover, the fine structure of the GaP band is resolved, namely peaks at 1.93 and 2.1 eV. However, the intensity of the emission in this case is much weaker, as compared with the PL intensity of the composite under the 2.71 eV line, because of the inefficient excitation.

Whatever the origin of the photoluminescence, the emission of the light from the semiconductor-coated opals is strongly modified in the frequency range covered by the photonic

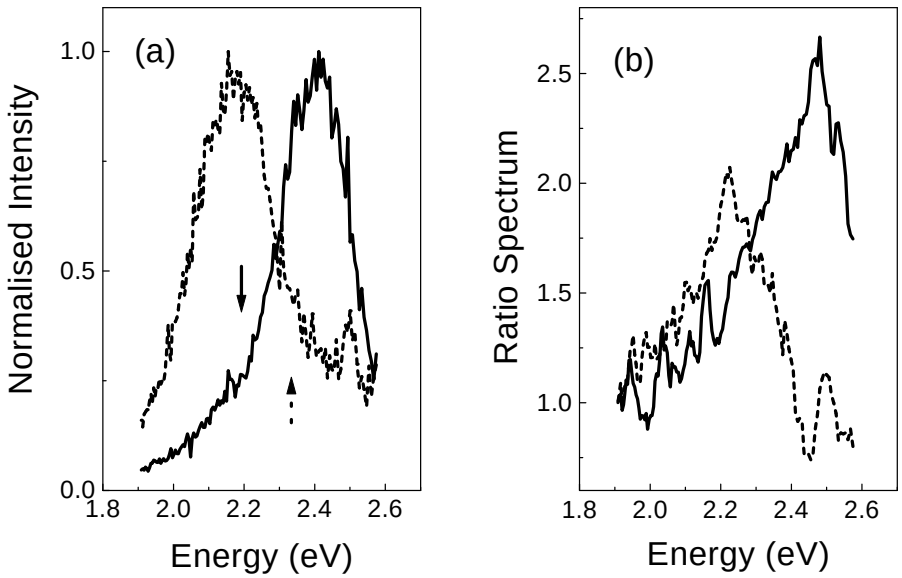

Figure 5. (a) Normalized PL spectra of GaP-opal ($f_{GaP} = 3.2\%$, $f_{SiO_2} = 0.87$) at $\theta = 0^\circ$ (solid line) and 20° (dotted line) under 2.71 eV excitation. (b) Ratio spectra for the same angles for a 2.5-fold increase in the pumping intensity. Spectra are normalized to the value outside the PBG energy range.

bandgap, when compared with the free-space-like emission. In air-opal a dip has been observed at the frequency of the stop-band (figure 6(b)). If the angle of collection of the light is changed, this dip crosses the emission band (see [19]). In contrast, the suppression of the emission in GaP-opal appears as the cut-off of the emission into regions on either side of the stop-band. This difference is the straightforward consequence of the stronger overlap of the stop-bands in GaP-opal as compared with air-opal.

The spontaneous emission rate relates directly to the density of photonic states [20] and therefore feedback between the electronic and photonic subsystems is produced in the photonic crystal [21]. In strongly anisotropic photonic crystals like air-opal, this effect is obviously small because the density of photonic states shows only a shallow minimum [8]. In coated opal the pseudogap becomes more pronounced as a result of the stronger overlap of the stop-bands. Correspondingly, the likelihood of a photon with energy in the PBG spectral region being emitted with an arbitrary wavevector decreases. Under continuous laser pumping this restriction means the redistribution of the emission output towards the edges of the photonic bandgap. Apart from the spectral re-distribution, the emission rate acquires directionality in space due to the anisotropy of the PBG structure. The extra level of emission intensity at the edge of the stop-band can be treated in terms of the amplified spontaneous emission (ASE). The spectrum of the emission rate was revealed by dividing the PL spectrum obtained at a high pumping level by that at a low pumping level. Figure 5(b) shows the ratio spectrum peak at the edge of the stop-band. The dependence of this peak position on the angle of collection of the light suggests strongly the PBG origin of this ASE band. The increased variation of the density of photonic states at the pseudogap in GaP-opal over that in air-opal has a pronounced effect on the magnitude of the change in the ratio spectrum. The lower incremental increase of the pumping power results in a much stronger variation of the emission rate in GaP-opal (figure 5(b)) as compared with air-opal (figure 6(c)).

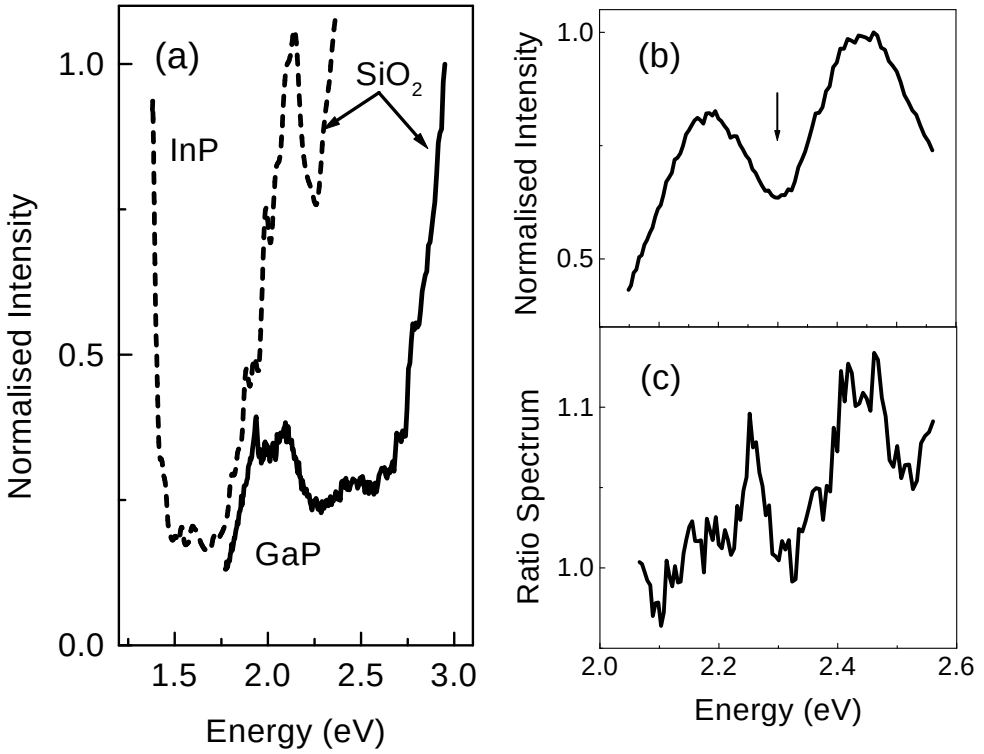

Figure 6. (a) Normalized PL spectra of InP-opal (dotted line) under 2.41 eV excitation and GaP-opal (solid line) under 3.53 eV excitation. (b) Normalized PL spectrum of air-opal under 2.71 eV excitation. (c) Ratio spectrum for air-opal for a 15-fold increase in the pumping intensity.

5. Conclusions

Photonic bandgap-like behaviour in opal has been improved by implementation of MOCVD processes for continuous coating of the inner surface of the opal voids with high RI semiconductor. A shift in the Bragg resonance and squeezing of its angular dispersion have been demonstrated for a high index coating, the thickness of which is less than 10% of the characteristic void size. Moreover, the thicker the coating, the wider the relative bandgap width and the better the stop-band overlap as compared with the air-opal. The variation of the relative bandgap width indicates the collapse of the stop-band when the RI of the coating-air shells matches the RI of the silica balls.

The impact of the bandgap upon the spontaneous emission from the photonic crystal appears stronger in GaP-opal than in air-opal. The stronger variation of the emission rate corresponds to the better overlap of the stop-bands for the same angular range of collection of the light in the coated opal.

Acknowledgments

This work was supported in part by the Leverhulme Trust (grant No F/179/AK), the Engineering and Physical Science Research Council (EPSRC grant No GR/M16542) and the Russian Foundation for Basic Research (grant 99-02-18156).

References

[1] See, for example, Rarity J and Weisbuch C (eds) 1996 *Microcavities and Photonic Bandgaps: Physics and Applications* (Dordrecht: Kluwer)
Soukoulis C M (ed) 1996 *Photonic Band Gap Materials (Nato ASI Ser. E 315)* (Dordrecht: Kluwer)
[2] Miguez H, Lopez C, Meseguer F, Blanco A, Vazquez L, Mayoral R, Ocana M, Fornes V and Mifsud A 1997 *Appl. Phys. Lett.* **71** 1148
[3] Vlasov Yu A, Astratov V N, Karimov O Z, Kaplyanskii A A, Bogomolov V N and Prokofiev A V 1997 *Phys. Rev.* B **55** R13 357
[4] Wijnhoven J E G J and Vos W L 1998 *Science* **281** 802
[5] Zakhidov A, Baughman R H, Iqbal Z, Cui C, Khayrullin I, Dantas A S O, Marti J and Ralchenko V G 1998 *Science* **282** 897
[6] Romanov S G, Fokin A V, Butko V Y, Tretiakov V V, Samoilovich S M and Sotomayor Torres C M 1996 *Phys. Solid State* **38** 1825
[7] Romanov S G, Johnson N P, Yates H M, Pemble M E, Butko V Y and Sotomayor Torres C M 1997 *Appl. Phys. Lett.* **70** 2091
[8] Busch K and John S 1998 *Phys. Rev.* E **58** 3896
[9] Moroz A and Sommers C 1999 *J. Phys.: Condens. Matter* **11** 997
[10] Yates H M, Flavell W R, Pemble M E, Johnson N P, Romanov S G and Sotomayor Torres C M 1997 *J. Cryst. Growth* **170** 611
[11] Miguez H, Blanco A, Meseguer F, Lopez C, Yates H M, Pemble M E, Fornes V and Mifsud A 1999 *Phys. Rev.* B **59** 1563
[12] Balakirev V G, Bogomolov V N, Zhuravlev V V, Kumzerov Y A, Petranovsky V P, Romanov S G and Samoilovich L A 1993 *Crystallogr. Rep.* **38** 348
[13] Smallwood A G, Thomas P S and Ray A S 1997 *Spectrochim. Acta* A **53** 2341
[14] Vos W L, Sprik R, von Blaadren A, Imhof A, Lagendijk A and Wegdam G H 1996 *Phys. Rev.* B **53** 16 231
[15] Tretyakov V V, Romanov S G, Fokin A V and Alperovich V I 1998 *Mikrochim. Acta* No S15, 211
[16] Bohrein G F and Huffman D R 1983 *Absorption and Scattering of Light by Small Particles* (New York: Wiley)
[17] Romanov S G, Fokin A V and De La Rue R M 1999 *J. Phys.: Condens. Matter* **11** 3593
[18] Romanov S G, Fokin A V, Alperovich V I, Johnson N P and De La Rue R M 1997 *Phys. Status Solidi* **164** 169
[19] Romanov S G 1998 *J. Nonlin. Opt. Phys. Mater.* **7** 181
[20] Purcell E M 1946 *Phys. Rev.* **69** 681
[21] John S and Quang T 1994 *Phys. Rev.* A **50** 1764